LASER INTERFEROMETER GRAVITATIONAL WAVE OBSERVATORY
--LIGO—
California Institute of Technology
Massachusetts Institute of Technology

Document Number: **LIGO- T020146-00-R** Date: 10/1/02

Authors: **Surjeet Rajendran**, Alan Weinstein

Topics in Data Analysis from Gravitational Wave Interferometers, including a Cross Correlation Statistic

This is an internal working note

of the LIGO Laboratory.

California Institute of Technology
LIGO Laboratory, MS 18-34
1200 E. California Blvd.
Pasadena, CA 91125
Phone (626) 395-3064
Fax (626) 304-9834

Massachusetts Institute of Technology
LIGO Laboratory, NW17-161
175 Albany St.
Cambridge, MA 01239
Phone (617) 253-4824
Fax (617) 253-7014

LIGO Hanford Observatory
P.O. Box 159
Richland, WA 99352
Phone (509) 372-8106
Fax (509) 372-8137

LIGO Livingston Observatory
P.O. Box 940
Livingston, LA 70754
Phone (225) 686-3100
Fax (225) 686-7189

Topics in Data Analysis from Gravitational Wave Interferometers, including a Cross Correlation Statistic to Identify Co-incident Bursts in LIGO

Surjeet Rajendran (Caltech)

Mentor: Dr. Alan Weinstein

LIGO REU SURF 2002

Final Report

Abstract

LIGO (Laser Interferometer Gravitational wave Observatory) seeks to open a new avenue to explore the universe by detecting gravitational radiation from extra-terrestrial sources. Gravitational waves from astrophysical sources can be broadly classified into four categories: bursts, chirps, periodic waves and stochastic waves. Bursts are emissions from localized sources in the sky whose precise waveforms are difficult to predict in advance, so that matched filtering techniques are not useful. The classical methodology adopted to detect bursts is to identify peaks of excess power in the sensitive frequency bands of the data stream and then localize the analysis around these peaks in order to rule out the possibility of the burst being the result of noise. This paper explores the possibility of using the coherence function (between the gravitational wave streams) as a statistic to further analyze the burst peaks. The paper also seeks to identify the optimal value of the coherence function statistic which minimizes the fake rate of detection while maintaining an acceptable level of efficiency of detection. This paper also seeks to quantitatively verify claims that the laser frequency noise and spacecraft displacement noise of the proposed LISA mission are suppressed using different combinations of measured quantities in time-delay interferometry.

Section 1: Introduction

(1) Interferometric Detectors of Gravitational Radiation

Interferometric detectors of Gravitational Radiation (of frequency content $0 < f < f_m$) use a phase modulated laser beam (of nominal frequency $\nu_0 >> f_m$) folded into several beams and, at one or more points where they intersect, monitor relative fluctuations of frequency or phase. These fluctuations are caused by frequency variations of the source of the electromagnetic waves about ν_0 as well as by relative motions between the source and the detector of the electromagnetic radiation.

General Relativity predicts that time variable gravitational fields between the source and the detector causes relative motion between them. Gravitational waves are an important example of time-variable gravitational fields and the net effect of a plane gravitational wave on space-time is to induce a strain in the plane orthogonal to its direction of propagation. Thus, Interferometry enables us to detect these strains as frequency fluctuations of the electromagnetic radiation circulating in the detector.

The sensitivity of an interferometer at a given frequency is determined by the strength of the coupling between the gravitational radiation and the proof-masses (ie: the free masses whose separation is altered by gravitational radiation, the change being detected through interferometry) at that frequency as well as by the expected power of the noise sources at that frequency. The regions of maximal sensitivity of terrestrial and space-based interferometers are therefore very different. Seismic noise determines the low frequency limit of sensitivity to terrestrial interferometers while acceleration noise of the proof-masses determines the same limit in the case of space-based interferometers. The net effect of the gravitational radiation on the arm lengths of the interferometer decreases when the wavelength of the gravitational wave becomes comparable

to, or smaller than, the arm lengths of the interferometer (due to the change in the polarity of the wave as it passes through the arms). This effect combined with shot noise determines the high frequency limit of sensitivity to both terrestrial and space-based interferometers. Several terrestrial interferometers like LIGO (Laser Interferometer Gravitational wave Observatory) (1) have been successfully built and are expected to be fully operational by 2004. LISA (Laser Interferometer Space Antenna) (2) is a proposed space-based interferometer which is expected to be launched within a decade.

(2) Antenna Patterns of an Interferometer

The Antenna Pattern of an interferometer is a function which when represented as a function of the polar and azimuthal angles gives the response of the interferometer to a gravitational wave incident on the interferometer from the direction of the unit vector specified by the given polar and azimuthal angles. The response of the interferometer is normally expressed as the difference between the arm lengths of the interferometer (called the Differential Mode or DTM). The sum of the two arm lengths (called the Common Mode or CTM) and the lengths of individual arms (ETMx, ETMy modes) are also useful characterizations of the interferometer response. In section (2) of this paper, we will calculate the antenna patterns (DTM, CTM, ETMx, ETMy modes) of an interferometer as a function of the angle (θ) between the arms. The antenna patterns for the special cases of $\theta = 90^o$ (the angle between the arms of LIGO) and $\theta = 60^o$ (the angle between the arms of LISA) are plotted.

(3) Gravitational Wave Bursts

Gravitational radiation from astrophysical sources can be broadly classified into four categories: bursts, chirps (created due to the coalescence of compact binaries), periodic waves (caused due to rotating neutron and binary star systems) and stochastic waves (primarily from the Big Bang). Bursts can be caused by the collapse of a star into a neutron star or black hole, the fall of stars and small black holes into supermassive black holes as well as asymmetric supernova explosions. The waveform of a gravitational wave burst caused due to these sources depends primarily on the dynamics of the system and therefore, burst waveform templates are difficult to create. Matched filtering techniques cannot therefore be reliably employed to detect bursts. The classical methodology adopted to detect bursts is to identify peaks of excess power in the sensitive frequency bands of the data stream. The LIGO Data Analysis System (LDAS) (3) identifies bursts in the data streams by using algorithms in the LIGO Analysis Library (LAL) (11) (like Power, Slope and TFClusters) which look for such peaks in the data stream from one detector, and then to find coincidences in time between such peaks in multiple detectors. However, excess

power in a particular frequency band may also be due to unexpected surges in the noise sources, for example, a glitch in the pre-stabilized laser may lead to excess power being generated at a particular frequency. In section (3) of this paper, we will discuss a statistical test that can be used to rule out such fake detections.

(4) Simulation of Time Delay Interferometry with applications in canceling laser frequency noise and space-craft motion effects in LISA:

The proposed LISA mission is currently envisaged as three spacecraft in heliocentric orbits with the orbital motion of the center of the constellation trailing the orbital motion of the Earth by 20^{o}, with the plane of the constellation being inclined at 60^{o} to the ecliptic (4). The orbits are designed such that the constellation is approximately equilateral (of side 5,000,000 KM) during the course of the mission. However, the dynamics of the spacecraft are such that it is impossible to maintain precisely equal arm lengths between them. The frequency fluctuations of the laser beams (about the nominal frequency ν_0, which for LISA is approximately 300 THz) are therefore not cancelled by the geometry of the interferometer. LISA will use a diode pumped Nd:YAG laser which offers a frequency stability of a few parts in 10^{-13}. However, since the goal of LISA is to detect gravitational waves which are expected to cause frequency fluctuations of the order of 10^{-20}, it is essential that the laser frequency fluctuations are precisely cancelled (or at least cancelled to the second order) in order for the interferometer to be able to detect gravitational waves. Armstrong, Tinto and Estabrook have proposed (in papers (5), (6) and (7)) several combinations of the LISA data which eliminates laser frequency fluctuation noise as well as the velocity noise caused due to the random motions of the optical benches of the LISA spacecraft. In Section (4) of this paper, the details and the results of a

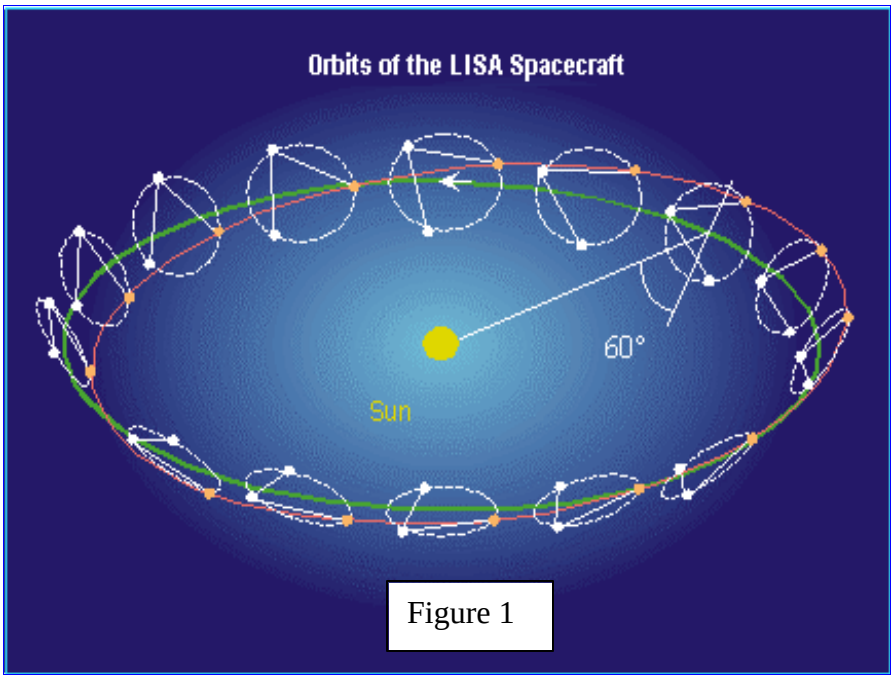

Figure 1

simulation of Time Delay Interferometry is presented. The results are found to be in accordance with the predictions made by Armstrong et al.

Section 2: Antenna Patterns of an Interferometer

Consider the co-ordinate system described in the adjoining figure (Figure 2). Let a plane gravitational wave (of dimensionless strain h), propagating along the Z-axis, be incident on the XY plane such that its net effect (up to first order in h) is to maximally alter lengths along the directions of the X and Y axes (such a wave is said to be in the "+" polarization). When such a gravitational wave passes through the XY plane, it takes the vector $\boldsymbol{v} = X\boldsymbol{i} + Y\boldsymbol{j} + Z\boldsymbol{k}$ to the vector $\boldsymbol{v'} = (1+h)X\boldsymbol{i} + (1-h)Y\boldsymbol{j} + Z\boldsymbol{k}$ (for a time duration very much smaller than the time period of the gravitational wave) (8). Therefore, when such a gravitational wave passes through this system, it takes the vector $\boldsymbol{OP}$ to $\boldsymbol{OP'}$ such that, if $|\boldsymbol{OP}| = r$ then, $|\boldsymbol{OP'}| = r(1 + h\mathrm{Sin}^2\phi\mathrm{Cos}2\theta)$. Since we know the effect of such a gravitational wave on an arbitrary vector, we can easily calculate the response of the interferometer arms by calculating the appropriate values of ϕ and θ of the interferometer arms (this calculation follows from simple geometry). The responses of interferometer for the cases where the angle between the arms is 90^o and 60^o were then plotted by using Mathematica. The results have been summarized below.

Figure 2

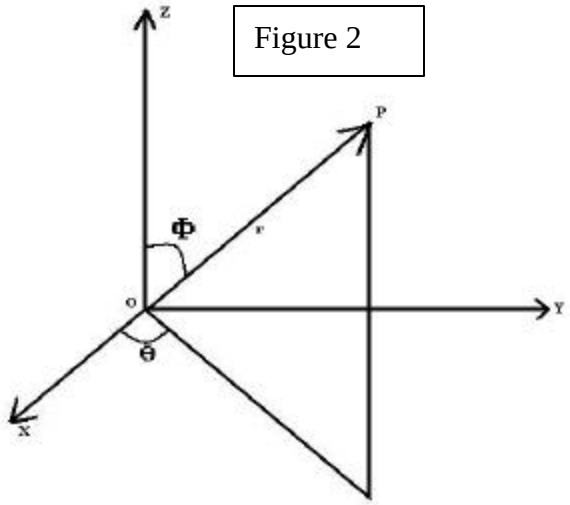

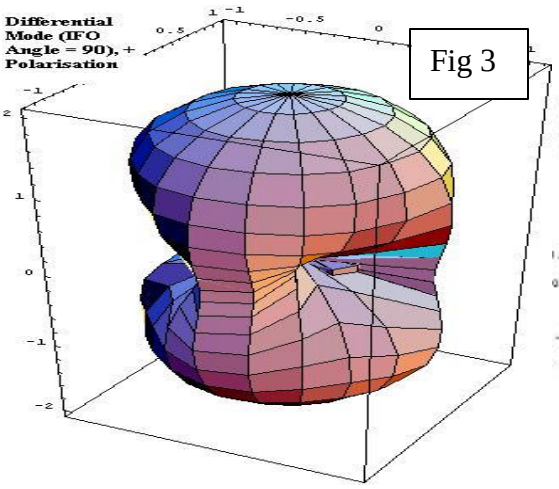

Fig 3

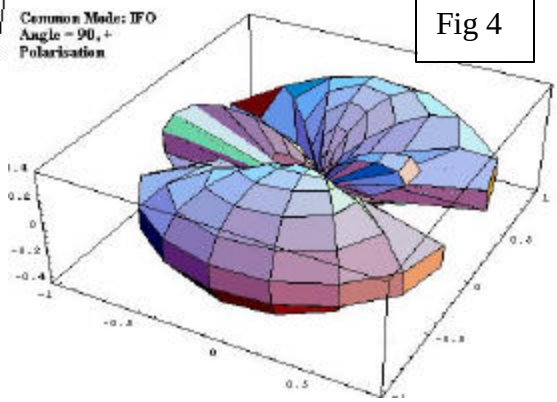

Fig 4

Differential Mode (IFO Angle 60), + Polarisation

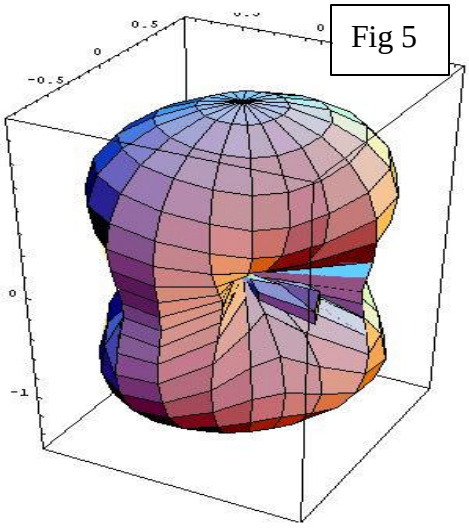

Fig 5

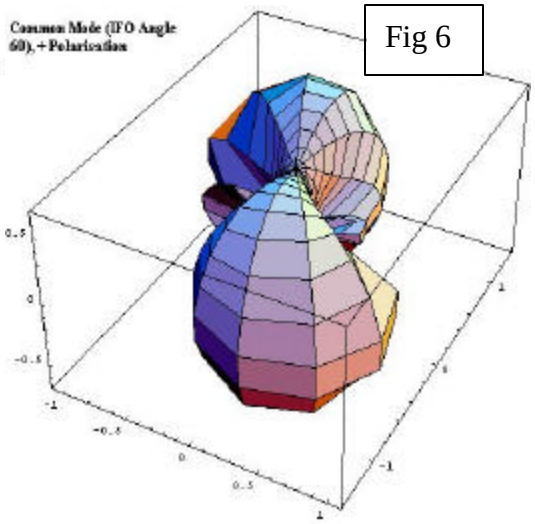

Fig 6

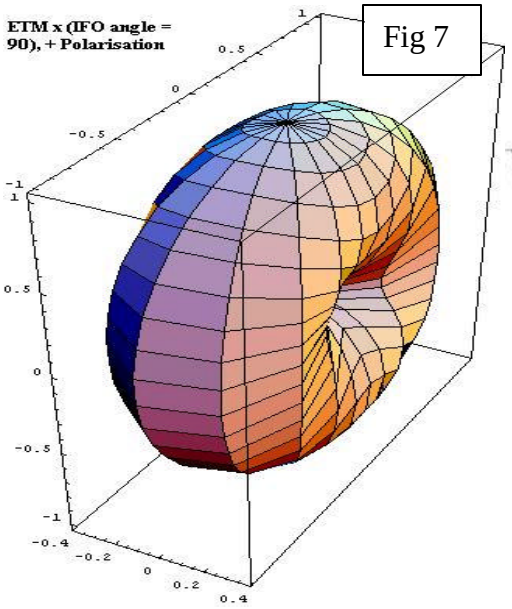

Fig 7

Fig 8

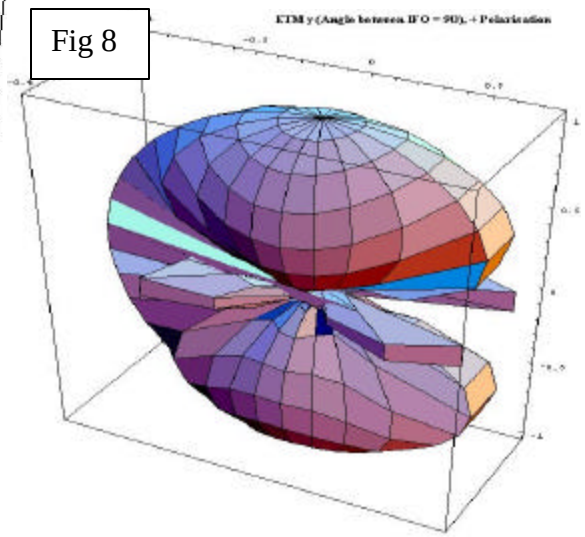

Section 3: Analysis of Co-incident Gravitational Wave Bursts

The software running in the LDAS system (3) identifies sections of the data stream which may contain gravitational wave bursts by looking for unexpected surges in the power of the data stream at sensitive frequencies. These identifications are performed by algorithms like the Power Event Trigger Generator (ETG) (11), the Slope ETG and the TFCluster ETG. When a burst-search ETG identifies a particular data section as "bursty", it generates a trigger containing useful information about the burst (eg: the start time, duration and central frequency of the burst etc.). The triggers thus generated are then stored in a meta-database (usually an XML file). The traditional method to reduce the fake rate of detection is to identify coincident (after allowing for the 10 ms light travel time between Hanford and Livingston) triggers and thereafter impose further consistency conditions on the identified data sections (eg: we may require frequency overlaps between the identified data sections). The efficiencies of these methods of burst detection were evaluated using the data gathered from the LIGO interferometers during LIGO's Engineering Run 7 (E7) (9). The basic method adopted to evaluate the efficiency of burst detection of a particular algorithm is to inject simulated gravitational wave bursts (like the Zwerger Muller waveforms) into the LIGO data stream, process the data stream through the algorithm and check if the algorithm identifies the injected burst. We thus arrive at the efficiency of detection of that particular algorithm. A plot of the efficiency of detection of the TFClusters ETG against the distance between the Earth and various Zwerger Muller supernovae is given below.

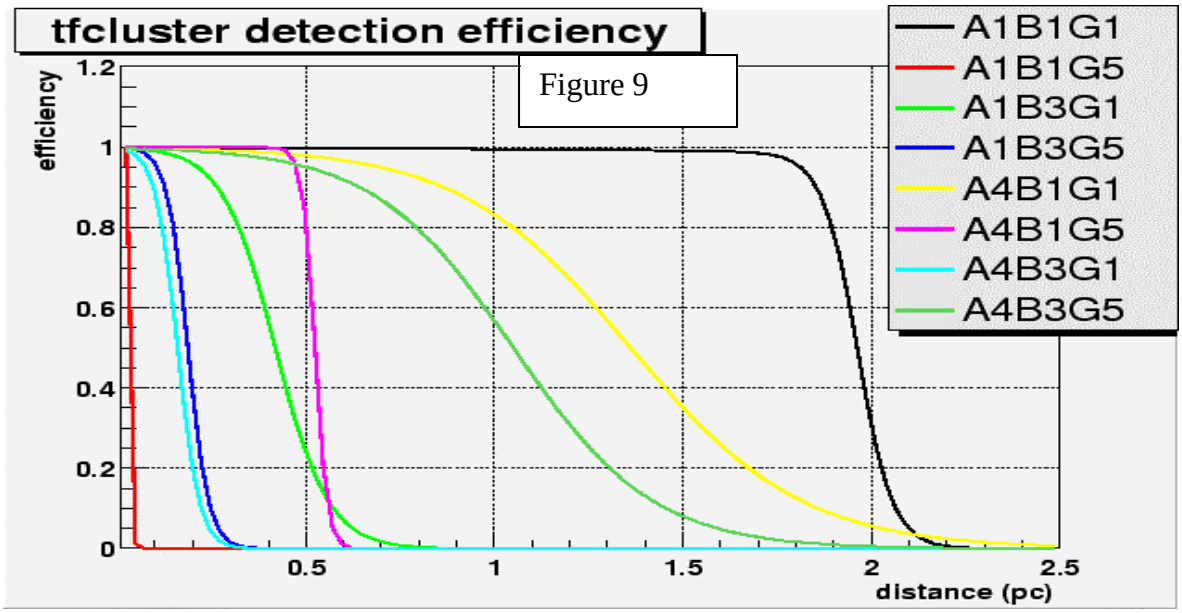

Figure 9 – (cf (10))

The accidental coincidence rate should be as small as possible; ideally, false coincidences should occur less than once per century. The coincidence rate depends on the thresholds used to define a burst event, and the coincident time-window. We desire to set these limits so that our efficiency for detecting real (or simulated) bursts remains high. With the settings used for analysis of the data from LIGO's E7 run, this false coincidence rate remains too high. Thus, we wish to explore the possibility of using the raw data from the interferometers to further reduce the fake rate while maintain a high efficiency. We therefore seek a statistical measure which significantly reduces the fake rate while maintaining very high efficiency for even the faintest injected burst which triggers the ETGs. We require this statistic to be robust even when the two interferometers have very different sensitivities (like the Livingston 4 KM Interferometer (L1) and the Hanford 2 KM Interferometer (H2)) as well as when there is a time delay of 10 ms (light travel time between H2 and L1) between the injected gravitational wave bursts. For this study, we focus on the data taken during the LIGO E7 run (December 28, 2001 through January 14, 2002), by the LIGO Livingston Observatory 4km detector (LHO4K, or L1), and the LIGO Hanford Observatory 2km detector (LHO2K, or H2). We have used data when both interferometers were "in lock" (capable of detecting gravitational waves), and which were pre-selected as a "playground" for the development of algorithms and the tuning of thresholds.

Let:

$X(t)$ = ΔT seconds of data from L1

$Y(t)$ = ΔT seconds of data from H2

$P_{L1}(f)$ = Discrete Power Spectral Density of X

$P_{H2}(f)$ = Discrete Power Spectral Density of Y

$C_{L1,H2}(f)$ = Discrete Cross Spectral Density of X, Y

$C_{XY}(f)$ = Discrete Coherence Function between X, Y

$= |C_{L1,H2}(f)|^2 / (P_{L1}(f) * P_{H2}(f))$

Consider the statistic:

$CCS = \Sigma\ CXY(f_i)\ \Delta f$ with $f_{min} <= f_i <= f_{max}$ (where the sum is over the frequency bins, as discussed below)

If the value of the CCS statistic when the data-streams X(t) and Y(t) contain gravitational wave bursts is significantly (statistically) different from the value of the CCS statistic when there are no coincident gravitational wave burst candidates in the data-streams X(t) and Y(t), then we can identify a gravitational wave burst candidate by demanding that the CCS statistic computed from the data-streams exceeds a certain threshold condition. We therefore estimate the distribution of the CCS statistic between the data-streams of L1 and H2 in the presence and in the absence of a simulated gravitational wave burst. We have determined a value of the CCS Statistic which can then be used to identify coincident gravitational wave bursts and reject accidental coincidences.

Parameters affecting the performance of the CCS Statistic:

(1) The value and performance (by which we mean its ability to distinguish a fake burst from a gravitational wave burst) of the CCS Statistic will depend upon the value of ΔT. If ΔT is a lot larger than the duration of the burst, then the CCS statistic will be dominated by the noise (thereby leading to a drop in performance) while if the value of ΔT is too small, we risk losing significant chunks of the gravitational wave burst signal thereby leading to a drop in performance. For our analysis, we take the value of ΔT = 1 second. The dependence of the CCS statistic on the value of ΔT needs to be explored.

(2) Δf will affect the value of the CCS statistic. But it should have little effect on the performance of the CCS statistic as a statistical tool to identify broad-band gravitational wave bursts. Δf merely acts as a blind magnifying factor for the CCS statistic in both cases. We used the value of Δf = 16 for our analysis.

(3) The value and performance of the CCS statistic also depends upon the range in frequency space over which we calculate the CCS statistic. This range is set by the values of f_{min} and f_{max}. The optimal values of this frequency band depend on the (a priori unknown) power

spectrum of the Gravitational Wave burst, compared with the power spectrum of the detector noise. In order to determine the optimal values of f_{min} and f_{max}, we plot the values of the coherence function $C_{l1,h2}(f)$ when there are no injected signals in the data-streams and compare it with the plot of $C_{l1,h2}(f)$ obtained when the data-streams contain simulated broad-band gravitational wave bursts. The value of f_{min} and f_{max} is then set by identifying the region in the frequency space where the plots are maximally different.

Comments on the playground data and simulated burst signals used for the analysis:

The data and triggers were obtained from the data gathered during E7. The simulated gravitational wave bursts were Zwerger-Muller supernovae (10) placed at a distance of 2 Parsec from the Earth (2 Parsecs being the limit of LIGO's sensitivity during E7 cf: figure 9). The data was whitened and resampled at 4 KHz before being analyzed. The resampling was primarily done because Zwerger-Muller supernovae have very low power over 1000 Hz and therefore, we have little to lose by discarding information about frequencies higher than 1000 Hz. The resampled data required less disk space, memory and cpu-time to process.

Determination of the values of f_{min} and f_{max} for Zwerger-Muller Supernovae at a distance of 2 Parsec:

The procedure previously outlined for determining the values of f_{min} and f_{max} was adopted in order to arrive at the optimal frequency range for various Zwerger-Muller supernovae. The following 7 plots show data from the same 1-second interval, into which 7 different ZM Supernova waveforms were added.

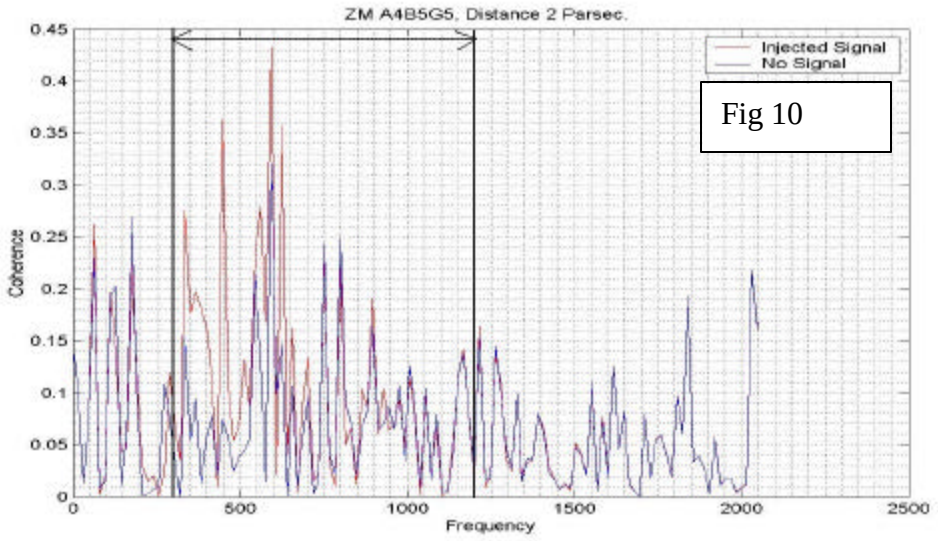

Fig 10

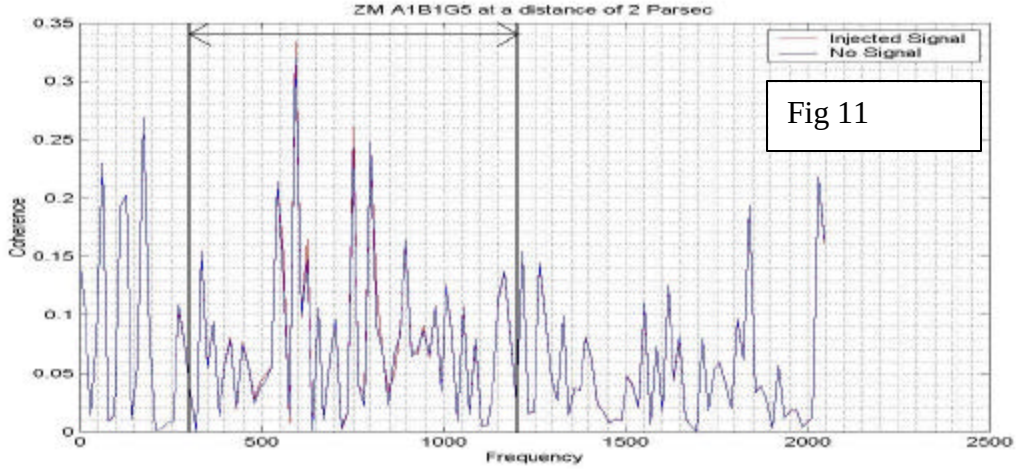
ZM A1B1G5 at a distance of 2 Parsec
Injected Signal
No Signal
Coherence
Frequency
0
0.05
0.1
0.15
0.2
0.25
0.3
0.35
500
1000
1500
2000
2500

Fig 11

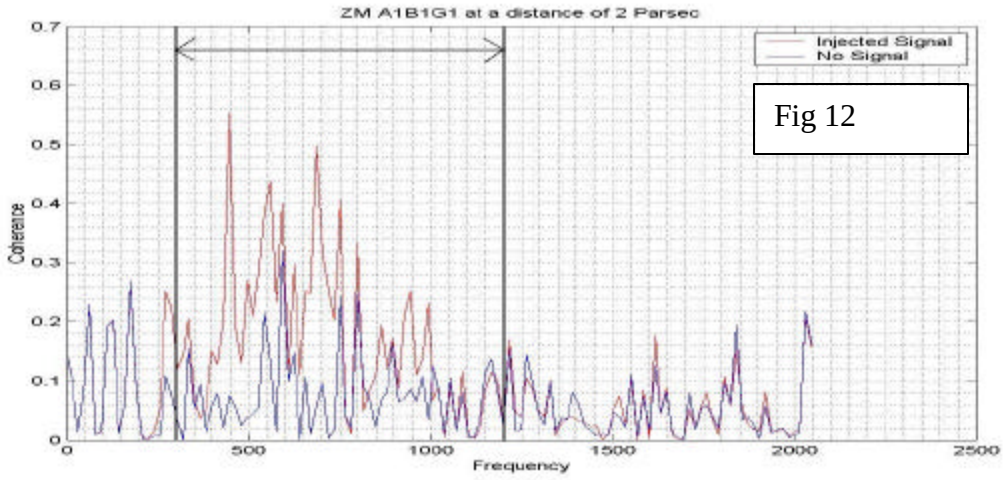
ZM A1B1G1 at a distance of 2 Parsec
Injected Signal
No Signal
Coherence
Frequency
0
0.1
0.2
0.3
0.4
0.5
0.6
0.7
500
1000
1500
2000
2500

Fig 12

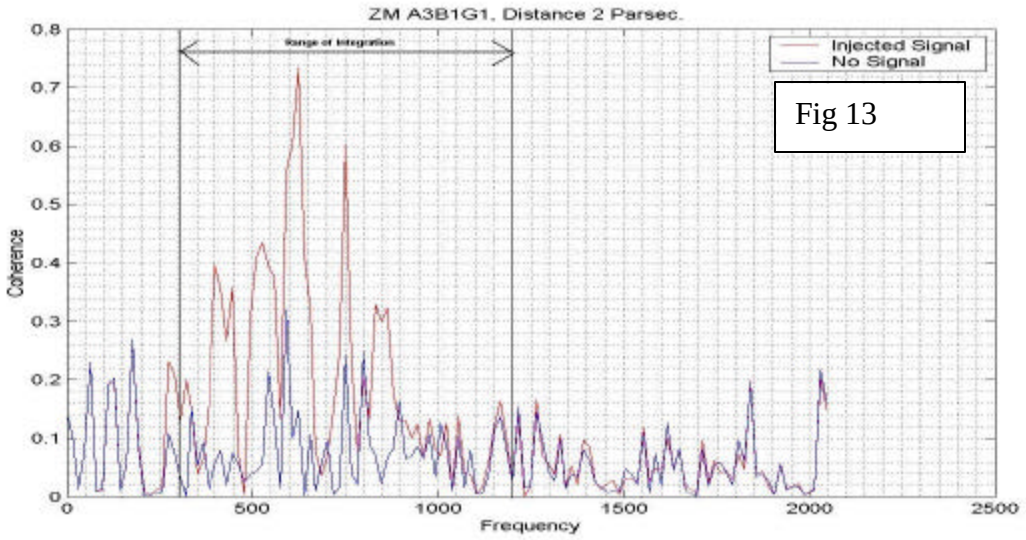
ZM A3B1G1, Distance 2 Parsec.
Range of Integration
Injected Signal
No Signal
Coherence
Frequency
0
0.1
0.2
0.3
0.4
0.5
0.6
0.7
0.8
500
1000
1500
2000
2500

Fig 13

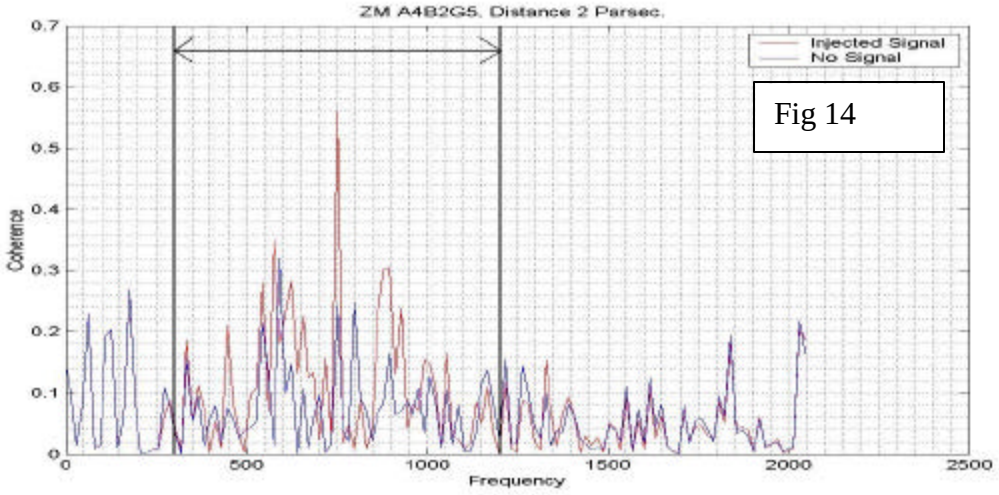
ZM A4B2G5, Distance 2 Parsec.
Injected Signal
No Signal
Coherence
Frequency
0
0.1
0.2
0.3
0.4
0.5
0.6
0.7
500
1000
1500
2000
2500

Fig 14

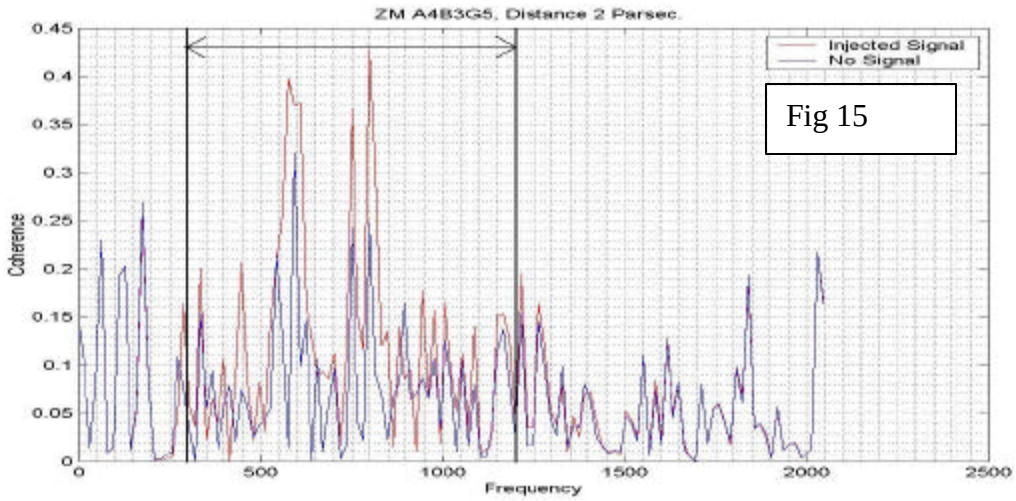

Fig 15

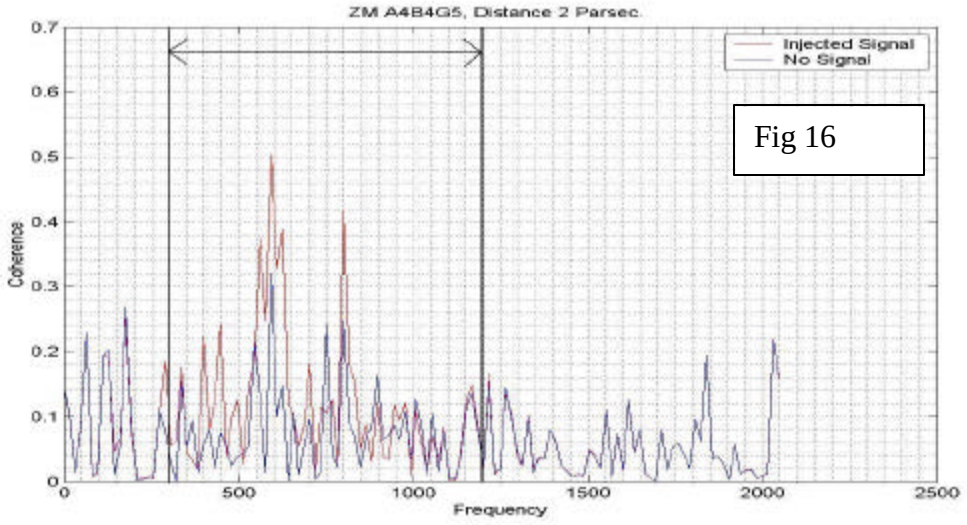

Fig 16

From the above plots (figures 10-16), it is clear that the region of interest lies between ~250 Hz – 1000 Hz. This is consistent with the fact that ZM supernovae have little power beyond 1000 Hz and the fact that LIGO has its peak sensitivity in this region. The plots also indicate that the CCS statistic will be of little use in detecting some weak waveforms (eg: A1B1G5). In fact, this seems to be the case for nearly 55 of the 78 ZM waveforms (the supernovae are placed at a distance of 2 Parsec). The values of f_{min} and f_{max} for our analysis were chosen to be 300 Hz and 1200 Hz respectively. This was done to include

all the significant peaks in the coherence function plots. The plots also indicate that by choosing a lower value of f_{max}=1000 Hz, the statistic will yield better results.

Procedure adopted to estimate the distribution of the CCS statistic in the presence and absence of a simulated Gravitational Wave Burst:

(1) We take N (N = 1800 for this study) seconds of data from L1 and H2. ΔT was taken to be 1 second. We then estimate the distribution of the CCS statistic on the raw data (in the absence of simulated gravitational wave bursts) by forming $(N/\Delta T)^2$ coincidences between them and computing the CCS statistic between the ΔT second intervals thus generated. We histogram the results to arrive at the distribution of the CCS statistic on the raw data.

(2) Since the CCS statistic test will be used only on the data sections that trigger the ETGs, we perform the same analysis on the "bursty" data sections between the times t and t + ΔT where t corresponds to the time identified by the ETG as the start time of the burst which triggered the tfClusters ETG.

(3) We then inject Zwerger-Muller waveform signals in the $(N/\Delta T)$ intervals (both bursty and non-bursty) of length ΔT. The distribution of the CCS statistic after signal injection is similarly studied. We then inject the Zwerger-Muller waveform signals with a time delay of 10 ms (H2/L1 light travel time) between them and estimate the CCS statistic by the above method. The results are plotted below:

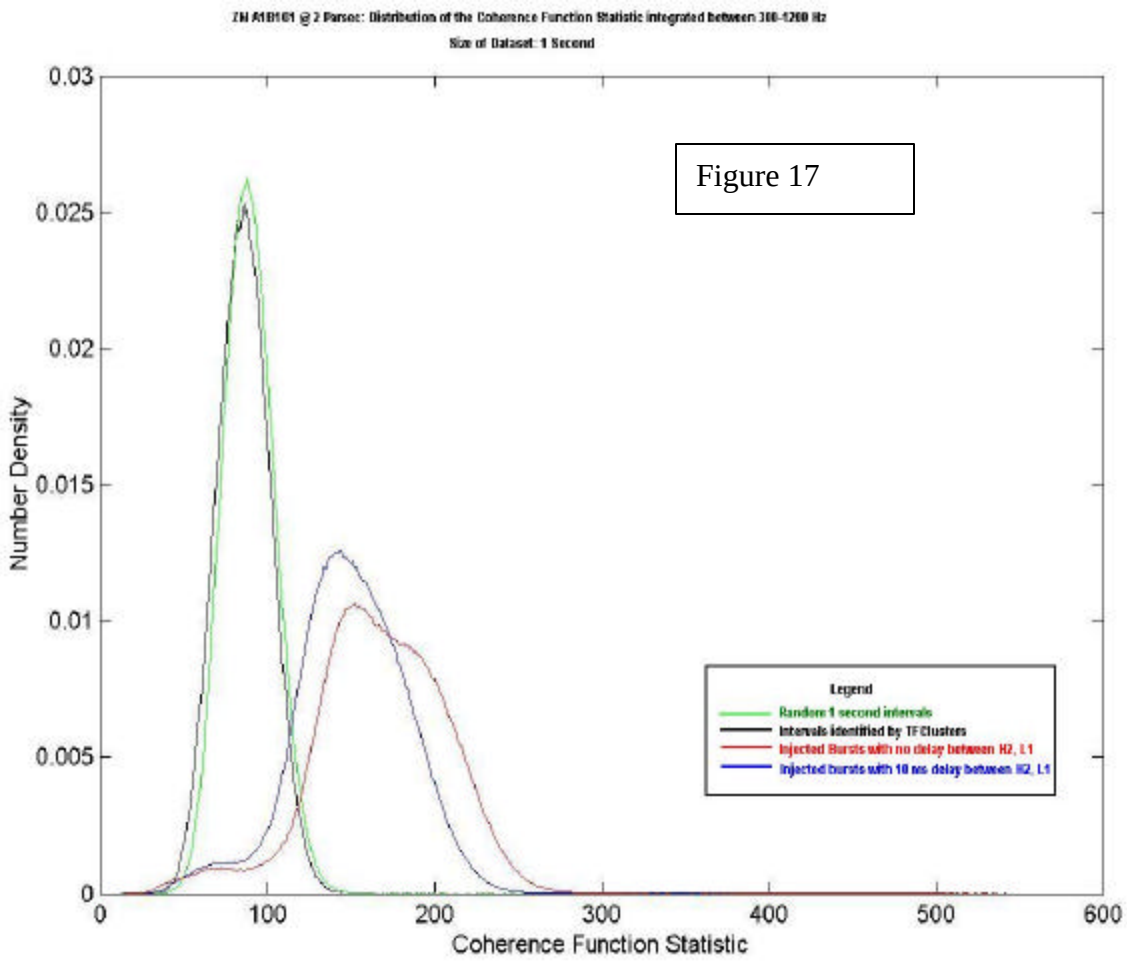

Figure 17

Comments on the Plots:

(1) It is clear from the comparison of the green and the brown curves (random intervals and intervals selected by tfClusters) that the distribution of the CCS statistic on the data sections identified by the ETGs as containing bursts is very similar to the distribution of the CCS statistic on random ΔT seconds of data from L1 and H2. Also, the distribution of the CCS statistic for intervals in which a barely-detectable ZM burst was injected peaks significantly higher than those intervals in which no simulated burst was injected.

(2) The peak of the CCS statistic distribution when the signal between H2, L1 is delayed by 10 ms occurs at a slightly lower bin than the peak of the distribution when there is no delay. However, we notice that we can produce an efficient value of the CCS statistic which maintains high rates of efficiency while minimizing the fake rate.

(3) The Matlab function *cohere (X, Y, NFFT, Fs)* (wherein, X, Y = data sampled at a rate of Fs Hz while NFFT controls the frequency resolution of the coherence estimate) was used

to estimate the coherence function. Since we are interested in a specific region of the frequency spectrum (namely, 300-1200 Hz), we must ensure that the coherence function estimate contains significant information between the frequency bins 300-1200 Hz. In order to achieve this, we require to maintain the ratio length(X)/NFFT = 16. If the ratio is bigger than 16, then the number of frequency bins in the coherence function estimate between 300-1200 Hz is far too small to cause a significant difference in the estimation of the CCS statistic. If the ratio is lesser than 16, the coherence function estimate between X, Y gets artificially boosted up due to the inadequacies of the Welch's averaged periodogram method of estimating the coherence function of a discrete time series when the size of the data sample is not large enough (as compared to NFFT).

Performance of the CCS Statistic:

From the above plots, a simple test to identify coincident gravitational wave bursts is to check if the value of the CCS statistic exceeds a given threshold value. If it exceeds the specified threshold, then we conclude that the coincident burst is consistent with originating from a coherent source (presumably, an extra-terrestrial gravitational wave). The value of the threshold should be chosen such that it operates at a low fake rate while maintaining high levels of efficiency. The fake rate has been plotted against the corresponding efficiency for the CCS statistic test in the following plots. The plots were made for Zwerger Muller A1B1G1 placed at a distance of 2 parsec from the Earth. This Zwerger Muller supernova was chosen because it represented the outer limit to the sensitivity of LIGO during E7 for the TFCluster ETG.

Figure 18

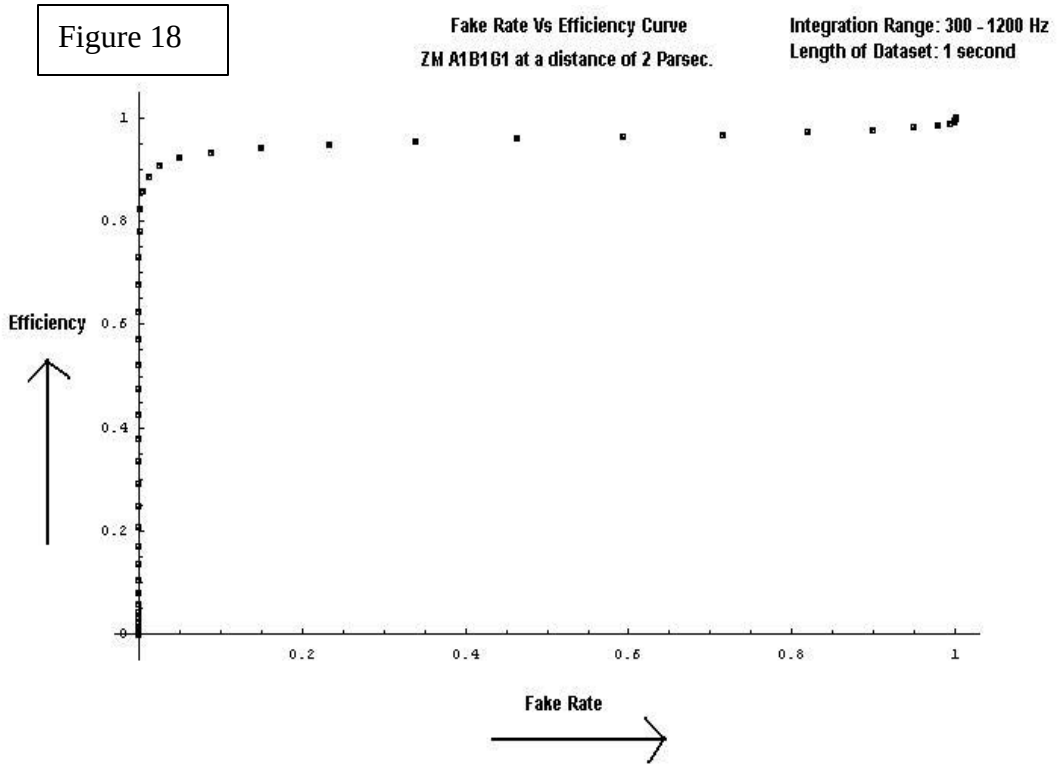

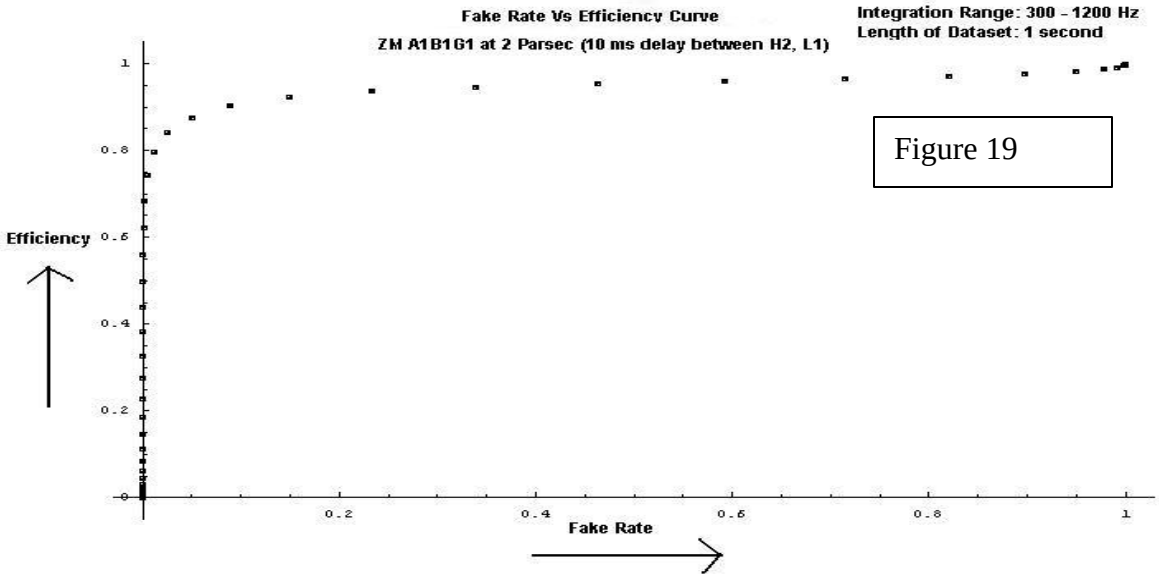

Figure 19

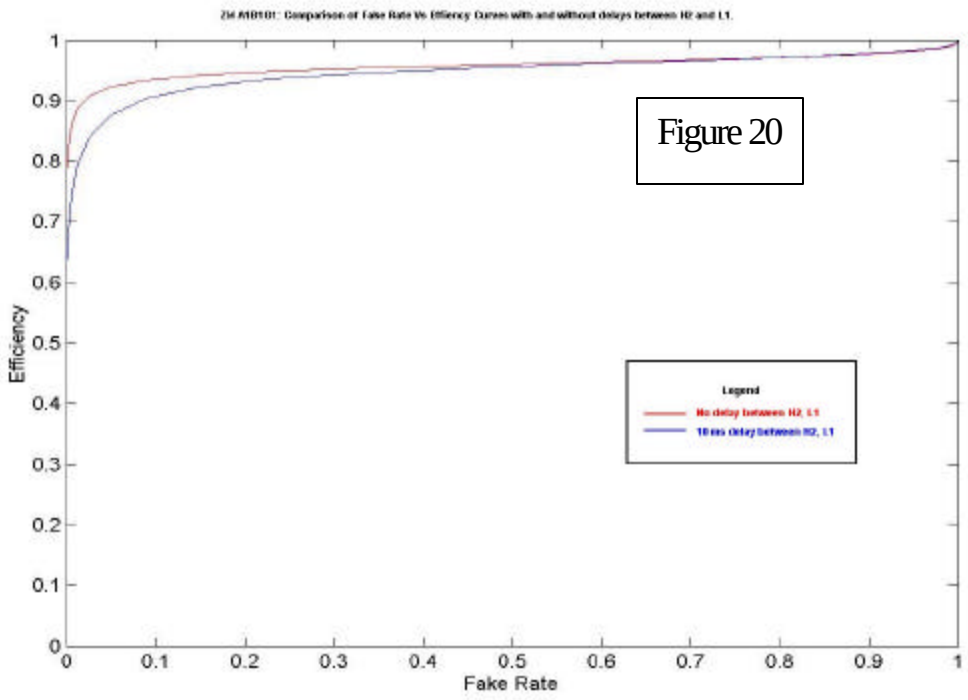

The above plots (figures 17-20) indicate that the CCS statistic test can be used to detect the faintest bursts which trigger the ETGs with an efficiency of nearly 70 percent while operating at close to a zero fake rate. The plots also indicate that we can increase the efficiency of the CCS statistic test by significant amounts if we allow for a marginal fake rate. The efficiency of detecting a Zwerger Muller of type A1B1G1 has been plotted against the distance between the supernova and the Earth. The plot is furnished below:

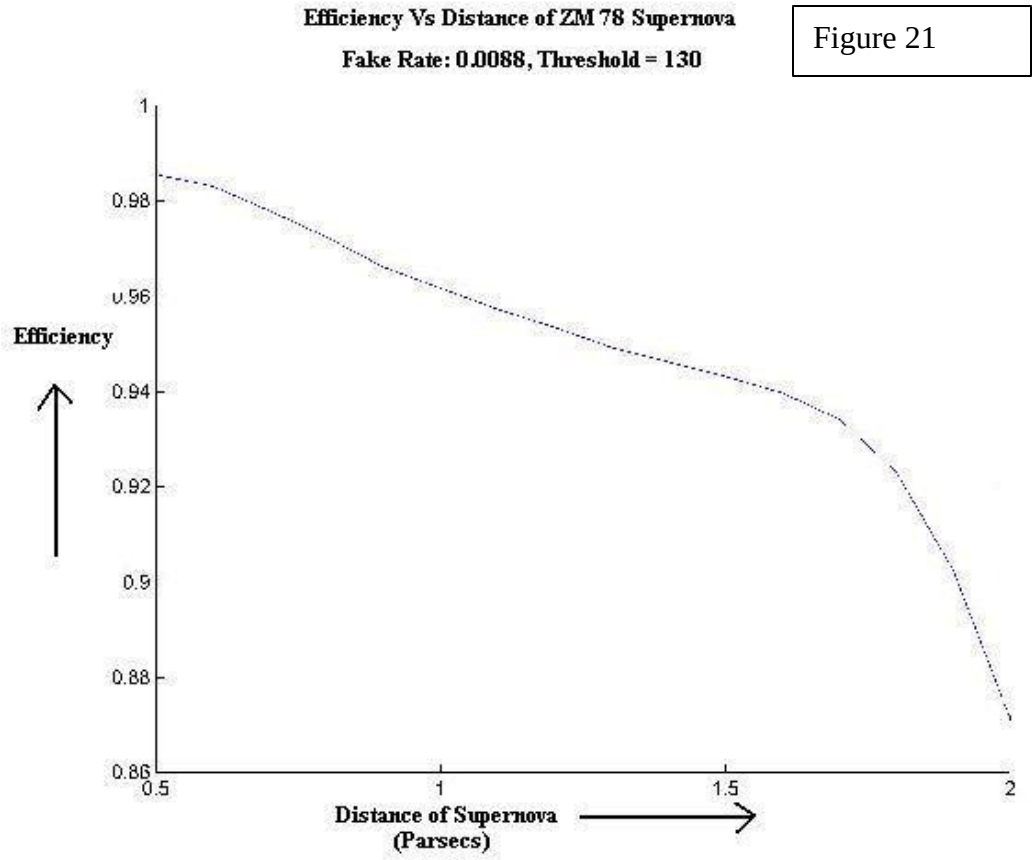

Figure 21

Conclusions:

The CCS statistic test proves to be a robust test for the detection of several types of Zwerger Muller waveforms. For the Zwerger Mullers, we identified the optimal values of f_{min} and f_{max} to be 250 Hz and 1000 Hz respectively. Since LIGO has its peak sensitivity in this particular region, we expect that these values would suffice for detecting all forms of gravitational wave bursts which have significant power in this particular section of the frequency space. The dependence of the CCS statistic on the waveforms must however be more closely examined to verify this conjecture. It is also important that we explore the dependence of the CCS statistic test on the duration (ΔT) of the data sections used while computing the CCS statistic.

Section 4: Simulation of Time Delay Interferometry in LISA

Description of the LISA System:

Consider the adjacent cartoon depicting the geometry of the LISA constellation (4). The spacecraft are labeled 1,2,3 and distances between pairs of spacecraft are L_1, L_2, L_3 with L_i being opposite spacecraft i. Unit vectors between spacecraft are $\boldsymbol{n}_i$, oriented as indicated in the figure. Each vertex spacecraft contains two rigid optical benches (the benches are attached to each other by an optic fiber) shielding two (almost) inertial proof masses. Each optical bench has its own laser, which is used to both exchange signals with one of the distant spacecraft and also to exchange signals with the adjacent optical bench. Thus, there are six optical benches, six lasers, and a total of twelve Doppler time series observed. The six beams exchanged between distant spacecraft contain the gravitational wave signal (plus noises); the other six beams are for comparison of the lasers and relative optical bench motions within each spacecraft. All beams are inertially referenced by reflection off a proof mass. An outgoing light beam transmitted to a distant spacecraft is routed from the laser on the local optical bench using mirrors and beam splitters; this beam does not interact with the local proof mass. Conversely, an incoming light beam from a distant spacecraft is bounced off the local proof mass before being reflected onto the photo-detector where it is mixed with light from the laser on that same optical bench. Beams between adjacent optical benches however do precisely the opposite. Light to be transmitted from the laser on an optical bench is first bounced off the proof mass it encloses and then directed to the other optical bench. Upon reception, it does not interact with the proof mass there, but is directly mixed with local laser light.

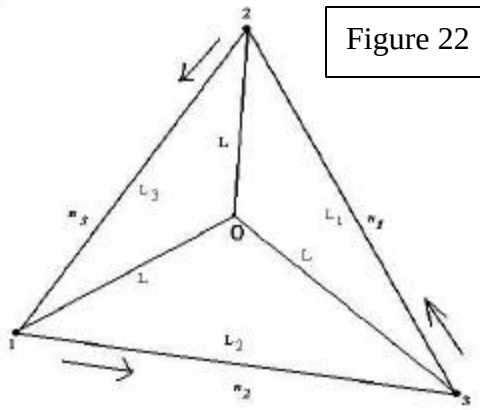

Figure 22

We adopt the following convention to index the Doppler data to be analyzed: Y_{31} is the fractional (or normalized by center frequency) Doppler series derived from reception at spacecraft 1 with transmission from spacecraft 2. Similarly, Y_{21} is the Doppler time series derived from reception at spacecraft 1 with transmission at spacecraft 3. The other four Doppler series from signals

exchanged between distant spacecraft (containing the Gravitational Wave signal) are obtained by cyclic permutation of the indices: 1->2->3->1. We also use a useful notation for delayed data streams: $Y_{31,23} = Y_{31}\ (t-L_2 - L_3)$ (where L_2 represents the light travel time between spacecraft 1 and 3 etc.). Six more Doppler series result from Laser beams exchanged between adjacent optical benches; these are similarly indexed as Z_{ij}. The fractional frequency fluctuations of the laser on the optical bench on spacecraft 1 which exchanges signals with spacecraft 2 is labeled C_1. The random velocity of this optical bench is labeled V_1 while the random velocity of the proof mass associated with this bench is labeled v_1. The fractional frequency fluctuations of the laser on the other optical bench on spacecraft 1 which exchanges signals with spacecraft 3 is labeled C_1* while the random velocity of this optical bench is labeled V_1* and the random velocity of the proof mass associated with this bench is labeled v_1*. The shot noise contribution to the Doppler time series Y_{ij} is denoted by Y_{ij}^{shot} , while the effect of a passing gravitational wave on the time series Y_{ij} is denoted by Y_{ij}^{GW}. Note that the shot noise contribution to the Doppler time series Z_{ij} is insignificant owing to the close proximity of the laser generating the beam and the photo-detector receiving the beam; and, the gravitational wave contribution to the Doppler time series Z_{ij} is similarly insignificant. The four photo-detector readouts at spacecraft 1, including gravitational wave signals and shot noises, are thus (the other time-series are arrived at by cyclic permutation of the indices: 1->2->3->1):

$$Y_{21} = C_{3,2} - n_2.\ V_{3,2} + 2n_2.v_1^* - n_2.V_1^* - C_1^* + Y_{21}^{GW} + Y_{21}^{shot}$$

$$Z_{21} = C_1 + 2n_3.(v_1 - V_1) - C_1^*$$

$$Y_{31} = C_{2,3}^* + n_3.\ V_{2,3}^* - 2n_3.v_1 + n_3.V_1 - C_1 + Y_{31}^{GW} + Y_{31}^{shot}$$

$$Z_{31} = C_1^* - 2n_2.(v_1^* - V_1^*) - C_1$$

Armstrong, Tinto and Estabrook have demonstrated in their papers (5), (6), (7) that this configuration enables us to combine the twelve Doppler time streams in such a manner that the combination eliminates laser frequency fluctuation noise and optical bench buffeting noises while retaining the gravitational wave signal. In this simulation of LISA, we simulated the response of the combinations X and α. The combination X is given by:

$$X = Y_{32,322} - Y_{23,233} + Y_{31,22} - Y_{21,33} + Y_{23,2} - Y_{32,3} + Y_{21} - Y_{31} +$$
$$(1/2) * (- Z_{21,2233} + Z_{21,33} + Z_{21,22} - Z_{21}) +$$
$$(1/2) * (Z_{31,2233} - Z_{31,33} - Z_{31,22} + Z_{31})$$

The combination α is given by:

$$\alpha = Y_{21} - Y_{31} + Y_{13,2} - Y_{12,3} + Y_{32,12} - Y_{23,13} -$$
$$(1/2) * (Z_{13,2} + Z_{13,13} + Z_{21} + Z_{21,123} + Z_{32,3} + Z_{32,12}) +$$
$$(1/2) * (Z_{23,2} + Z_{23,13} + Z_{31} + Z_{31,123} + Z_{12,3} + Z_{12,12})$$

Cyclic permutation of the indices of X (1->2->3->1) yields the combinations Y and Z while a similar permutation performed on α gives combinations β and γ.

Details of the Time Delay Interferometry Simulation

The simulation was written in Matlab. The noise spectra of the expected noise sources, the transfer function of the coupling of the LISA constellation to a passing plane gravitational wave as well as the noise canceling combinations of the LISA data were obtained from (4), (5), (6) and (7). The data for the simulation was generated and sampled at 2 Hz since LISA is maximally sensitive between 10^{-4} Hz – 1 Hz. Since we require a frequency resolution of at least 10^{-4} Hz, the simulation was executed to obtain a week (604800 seconds) of LISA data and the power spectrum of the gathered data in the combinations described above was then estimated. The simulation in its current state accepts only elliptically polarized sinusoidal gravitational waves (LISA sensitivities have been traditionally given for sinusoidal waves). In this particular simulation of LISA, we assume that the Doppler data received at each spacecraft has been preprocessed to remove Doppler shifts caused due to known orbital motion of the spacecraft. We also assume that the distances between the spacecraft (L_1, L_2 and L_3) are precisely known. In papers (4), (5), (6) and (7), Armstrong et al. have analyzed the precision required in measuring L_1, L_2 and L_3 so as to reduce the laser frequency fluctuation noise and spacecraft motion noise to second order and they find that the required precisions are easily attainable. Therefore, the assumption that the arm lengths of the constellation are precisely known is unlikely to cause significant errors. The simulation therefore deals with a system which consists of three almost but not precisely stationary spacecraft (ie: each spacecraft is assumed to have a small random velocity), the spacecraft forming the vertices of a triangle with known sides. The Doppler data represented in this simulation is normalized by central frequency (300 THz corresponding to 1 μm wavelength laser light from the Nd:YAG Lasers).

Generation of Noise with a given Frequency Spectrum

The following procedure was adopted to generate random signals (the noise) with a given power spectral density.

(1) Use Matlab's built-in randomizer to generate a normal random time series X(t).

(2) Compute the Fourier Transform of X(t) to obtain X(f).

(3) Theoretically, we expect X(f) = 1 (as X(t) is white gaussian noise). In order to obtain a random signal Y(t) with a power spectrum S(f), we form $Y(f) = X(f)*(S(f)^{1/2})$.

(4) Compute the inverse Fourier transform of Y(f) to obtain the random signal Y(t). It can easily be verified that the power spectrum of Y(t) is indeed S(f).

Results of the Simulation:

The simulation was executed to gather 1 week (604800 seconds) of LISA data and the power spectrum of the raw Doppler data as well as the power spectra of the noise canceling combinations α and X (see paper) were calculated. The sinusoidal gravitational wave used in the simulation was an elliptically polarized gravitational wave of dimensionless amplitude 10^{-21} incident on the LISA constellation from the point (π/4, π/4) on the celestial sphere with its co-ordinates on the Poincare sphere being (π/4, π/4). Plots of a typical time series of the raw Doppler data from the photo-detectors and the time series produced by the noise canceling combinations α and X as well as the corresponding power spectra have been plotted below:

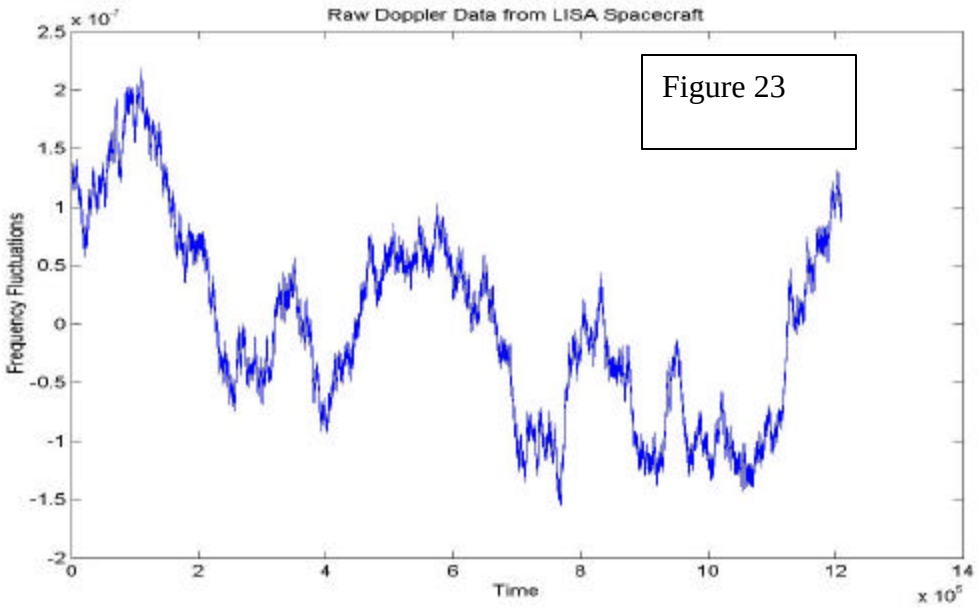

Figure 23

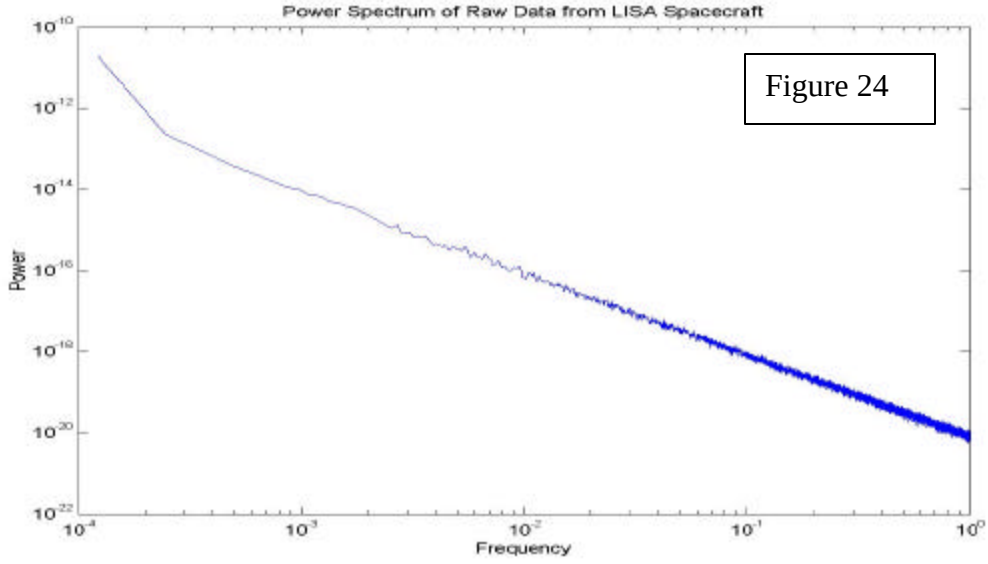

Figure 24

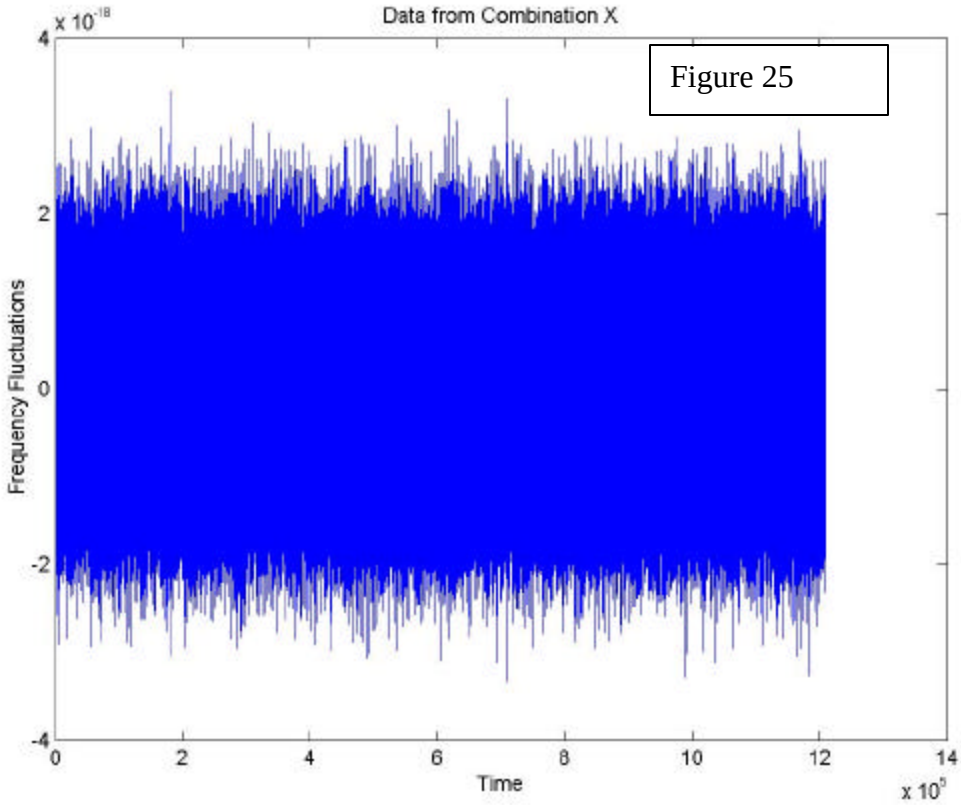

Figure 25

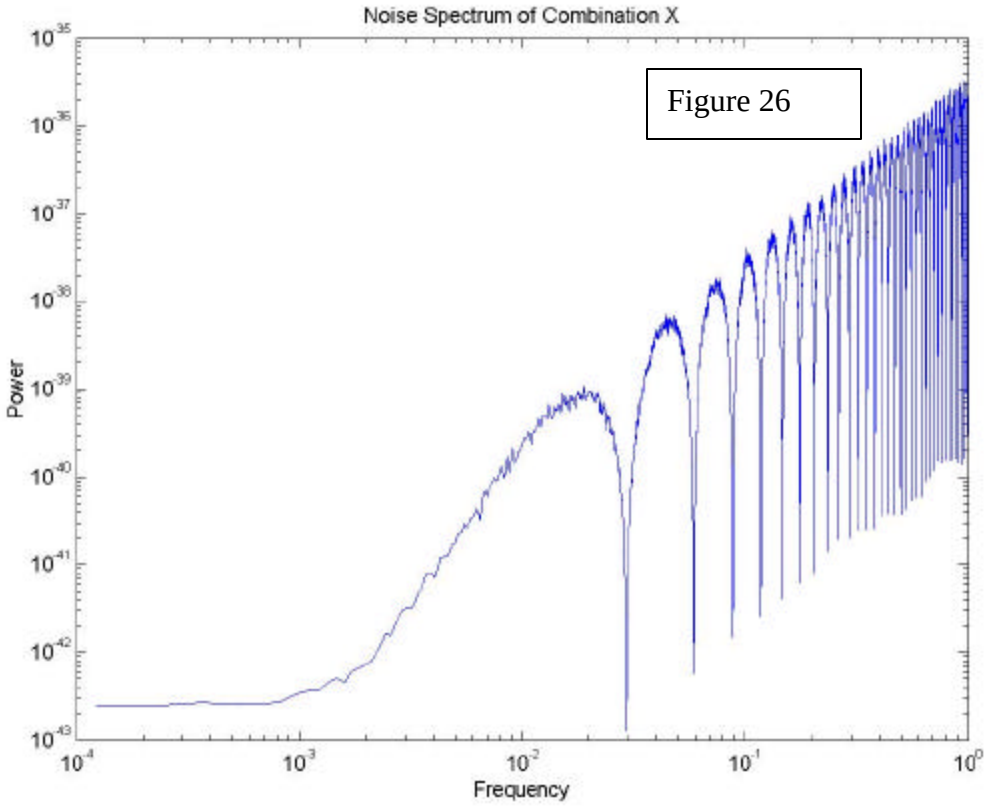

Figure 26

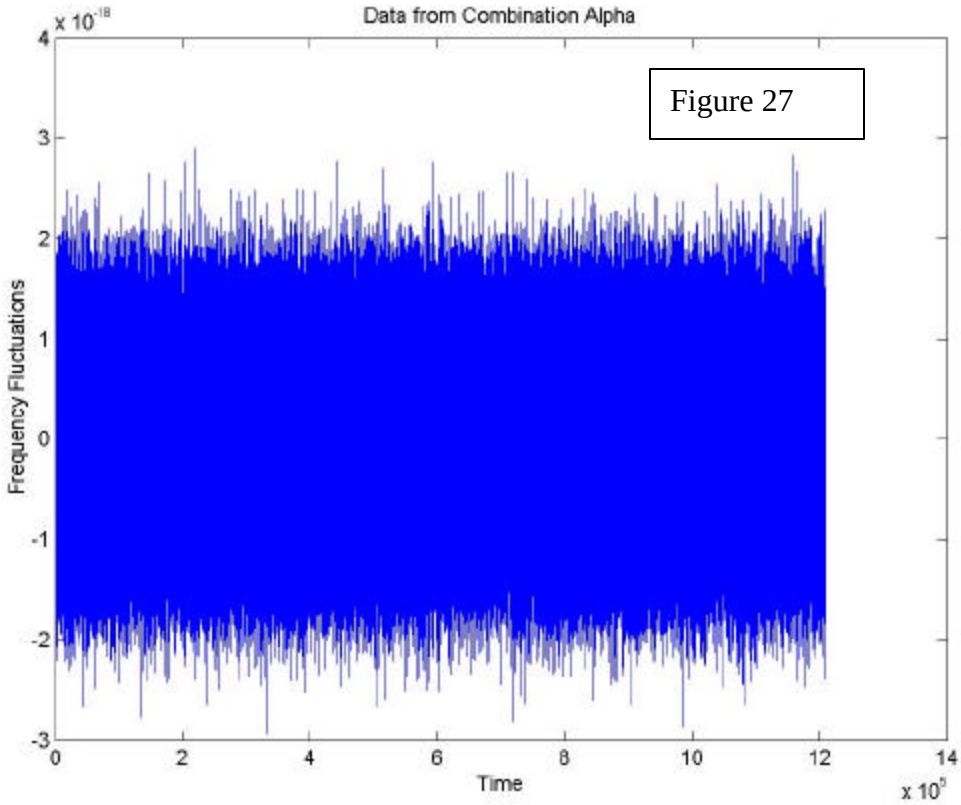

Figure 27

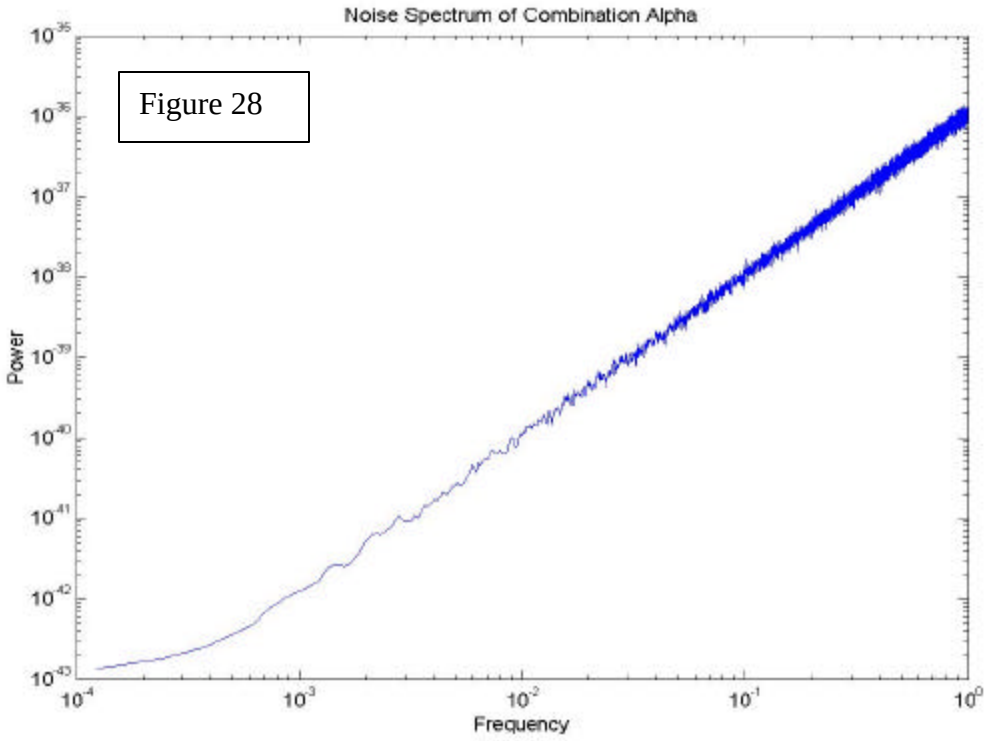

Figure 28

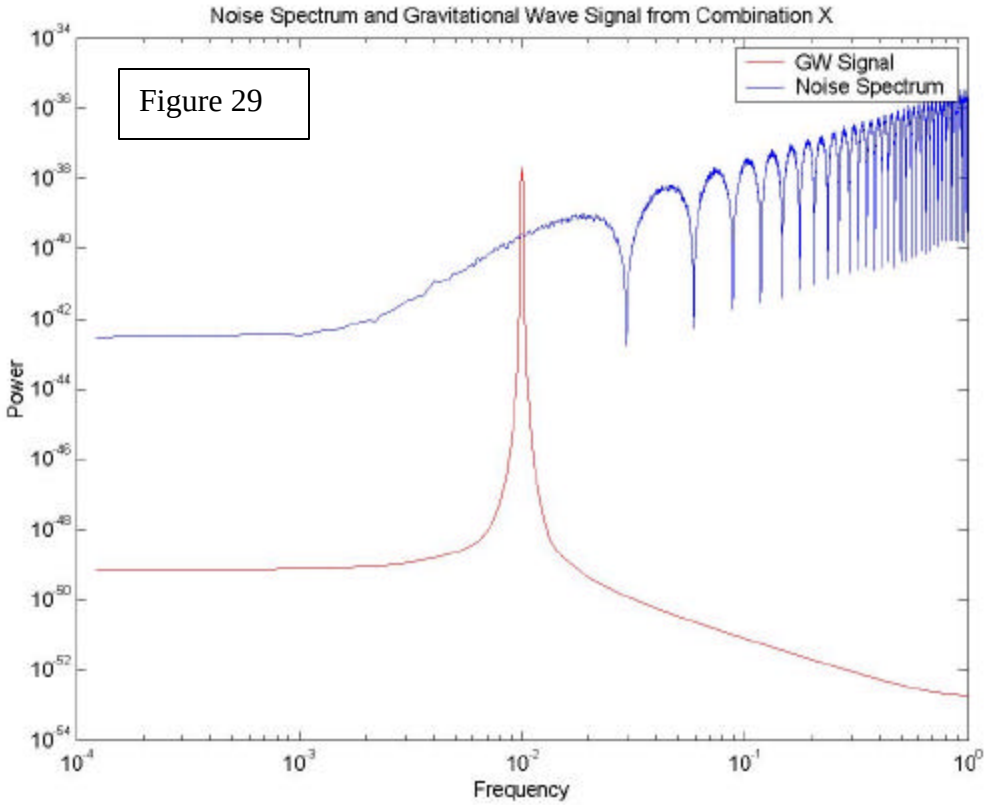

Figure 29

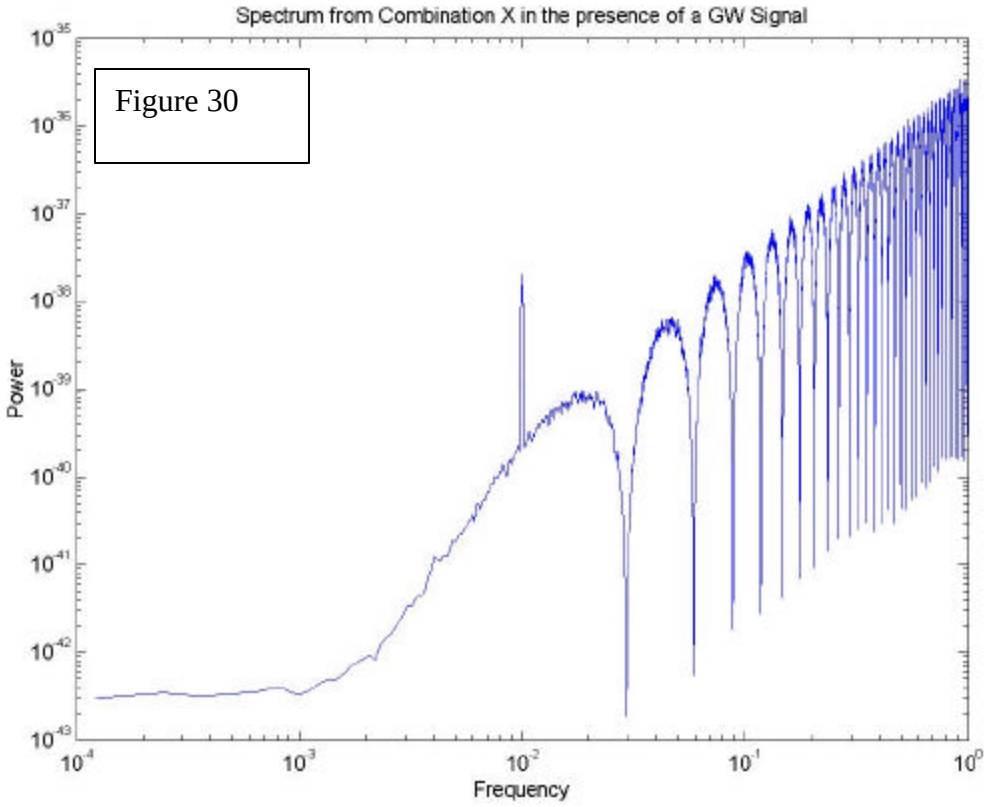

Figure 30

Conclusions:

The above plots (figures 23-30) demonstrate that the noise canceling combinations α and X successfully cancel the laser frequency fluctuation noise and spacecraft motion effects to acceptable levels while allowing us to detect the gravitational wave. The noise spectra obtained from the simulation are identical to the spectra obtained by Armstrong, Estabrook and Tinto (in papers (1), (2), (3)) through an analytic calculation of the appropriate transfer functions. Thus, the simulation quantitatively demonstrates that Time Delay Interferometry can be successfully implemented in LISA to recover the gravitational wave signal even when the system is swamped by laser frequency fluctuation noise and spacecraft motion effects. The gravitational wave sensitivity of LISA is then limited by acceleration noise (at low frequencies) and shot noise (at high frequencies).

Acknowledgements

I thank my mentor **Dr. Alan Weinstein** for having chosen me for this SURF. I have had several valuable discussions with him during the course of the summer and this SURF would not have been as enjoyable, edifying and successful as it was without his constant support and encouragement. This SURF was performed at the LIGO 40m Prototype Lab at Caltech as part of the NSF's REU and Caltech's SURF program.

References:

(1) *The LIGO Home Page* at: www.ligo.caltech.edu

(2) *The LISA Home Page* at www.lisa.jpl.nasa.gov

(3) *The LDAS Home Page* at http://www.ldas-cit.ligo.caltech.edu/

(4) *LISA Pre Phase A Report, Second Edition, 1998* by P. Bender et al.

(5) *Time-delay analysis of LISA gravitational wave data: Elimination of space craft motion effects* by F.B. Estabrook, Massimo Tinto and J.W. Armstrong, Physical Review D, Volume 62 042002.

(6) *Time-Delay inteferometry for space-based Gravitational Wave Searches* by J.W. Armstrong, F.B.Estabrook and Massimo Tinto, The Astrophysical Journal, 527:814-826, 1999 December 20

(7) *Cancellation of Laser Noise in an unequal-arm interferometer detector of gravitational radiation* by Massimo Tinto and J.W. Armstrong, Physical Review D, Volume 49, 102003

(8) *Fundamentals of Interferometric Gravitational Wave Detectors* by Peter R. Saulson, World Scientific Publishing Co.

(9) *LIGO Engineering Run 7* (http://blue.ligo-wa.caltech.edu/engrun/E7/)

(10) *Dynamics and gravitational wave signature of axisymmetric rotational core collapse* by T. Zwerger and E. Muller, Astronomy and Astrophysics (1997)

(11) *The LAL Homepage at* http://www.lsc-group.phys.uwm.edu/lal/

Signatures:

Dr. Alan Weinstein (Mentor):